THE JOURNAL OF PHYSICAL CHEMISTRY Letters

Letter

pubs.acs.org/JPCL

Explicit Differentiation of G-Quadruplex/Ligand Interactions: Triplet Excited States as Sensitive Reporters

Di Song, Wen Yang, Tingxiao Qin, Lidan Wu, Kunhui Liu, and Hongmei Su*

Beijing National Laboratory for Molecular Sciences (BNLMS), State Key Laboratory of Molecular Reaction Dynamics, Institute of Chemistry, Chinese Academy of Sciences, Beijing 100190, P. R. China

Supporting Information

ABSTRACT: We report a new transient spectral method utilizing triplet excited state as sensitive reporters to monitor and differentiate the multiplex G-quadruplex/ligand interactions in a single assay, which is a difficult task and usually requires a combination of several techniques. From a systematic study on the interactions of porphyrin (TMPyP4) with each telomeric G-quadruplex: $AG_3(T_2AG_3)_3$, $G_2T_2G_2TGTG_2T_2G_2$, $(G_4T_4G_4)2$, and $(TG_4T)4$, it is convincingly shown that the ligand triplet decay lifetimes are sensitive to the local bound microenvironment within G-quadruplexes, from which the coexisting binding modes of end-stacking, intercalation, and sandwich are distinguished and their respective contribution are determined. The complete scenario of mixed interaction modes is thus revealed, shedding light on the past controversial issues. Additional control experiments demonstrate the sensitivity of this triplet reporter method, which can even capture the binding behavior change as the G-quadruplex structures are adjusted by Na^+ or K^+.

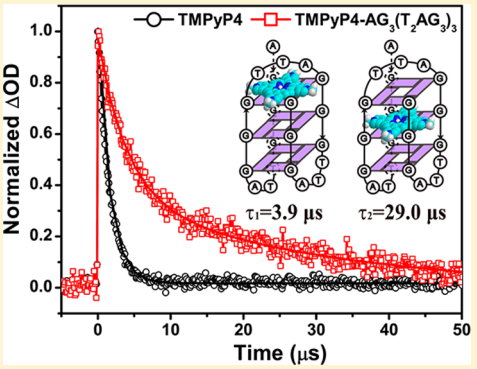

SECTION: Biophysical Chemistry and Biomolecules

G-quadruplexes are tetrastranded helical structures arising from the self-assembly of specific guanine-rich DNA sequences, which exist ubiquitously in the human genome including the telomere as well as promoter regions of certain oncogenes.[1] Recent studies demonstrate the formation of G-quadruplex structures not only in vitro,[2−5] but also in human cells.[6,7] Due to their participation in many key biological processes, particularly the ability to inhibit the activity of telomerase that is activated in most cancer cells, G-quadruplexes can act as tumor-selective targets for cancer treatment.[8,9] A large number of small molecules (the so-called ligands) can bind and stabilize G-quadruplexes, interfering with telomere replication.[10−14] These telomerase inhibitors are thus important because of their promising use as anticancer agents, and great interests have been sparked in the synthetic design of G-quadruplex ligands[10,11] and understanding of interactions between ligand and G-quadruplex.[12−14]

Because of high degree of structural polymorphism in DNA G-quadruplexes, one challenge in monitoring G-quadruplex/ligand interactions is to dissect the rich variety of the ligand binding sites and its modes of interaction.[12] A number of techniques have been used to address this issue and led to better understandings, including X-ray crystallography,[15] NMR spectroscopy,[16] isothermal titration calorimetry (ITC),[17,18] UV−vis,[19] circular dichroism (CD),[20] fluorescence spectroscopy,[21,22] and so on. However, current methods are generally sensitive to only one type of binding mode or site, and then it is difficult to simultaneously distinguish different ones in a single measurement. Usually more than one method is needed to obtain a complete picture, but a combination of different techniques is not always straightforward because sometimes the two techniques provide different results for the same G-quadruplex/ligand structure.[12] For example, for the ligand of porphyrin (TMPyP4) bound with the human telomeric sequence $AG_3(T_2AG_3)_3$,[17,19,22,23] although extensively studied by various methods,[17,19,22,23] its binding mode is still controversial, with no consensus to date.[12] In this context, an efficient and robust characterization methodology that can explicitly identify various binding modes and further quantify their respective contributions is highly desirable.

Herein, we report a new transient spectral method utilizing triplet excited state as sensitive reporters to recognize different binding sites and interaction modes in a single assay. Most of the G-quadruplex ligands are planar aromatic systems containing heteroatoms,[12] a feature that could result in high quantum yields of triplet states upon photoexcitation. Presumably, the decay dynamics of these triplet excited states are highly sensitive to the confined environment where the ligand binds to G-quadruplex, thereby they should make it possible to distinguish different binding sites and assess contributions of each binding mode. Previously, triplet excited states were used as reporters to probe the binding of drugs to proteins, which successfully determined binding sites and even assessed the distribution of a drug between two transport

Received: May 23, 2014
Accepted: June 13, 2014
Published: June 13, 2014

   dx.doi.org/10.1021/jz501040a | J. Phys. Chem. Lett. 2014, 5, 2259−2266

proteins present simultaneously in blood.[24,25] Nevertheless, to the best of our knowledge, there is hitherto no report of the use of triplet excited states to probe the interplay between G-quadruplexes and ligands.

In this work, we have examined the G-quadruplex/ligand interactions for porphyrin (TMPyP4), an effective inhibitor of human telomerase,[26] binding separately with four biologically relevant but distinct telomeric G-quadruplexes, that is, intramolecular basket-type $AG_3(T_2AG_3)_3$, intramolecular chair-type thrombin-binding aptamer $G_2T_2G_2TGTG_2T_2G_2$ (TBA), intermolecular dimer-hairpin-folded $(G_4T_4G_4)2$, and intermolecular parallel $(TG_4T)4$ (Figure S1, Supporting Information). By monitoring the triplet excited state decay dynamics, it is observed that TMPyP4 bound within G-quadruplexes follows a biexponential decay behavior, with two lifetime components markedly longer than free TMPyP4, due to the local bound microenvironment that prevents molecular oxygen access and triplet quenching. The coexisted binding sites are therefore allowed to be differentiated explicitly, and their respective contribution in the overall binding is determined. Further control experiments demonstrate the sensitive capture of the binding behavior variation induced by the structural change of G-quadruplexes. It shows here that the full scenario of mixed interaction modes can be revealed readily and clearly in a single assay, by using triplet excited state as a spectral reporter. This new method thus offers a straightforward platform that can be applied to monitor and differentiate the versatile and complex G-quadruplex/ligand interactions, which is a difficult task and usually requires a combination of several different techniques.

Steady-State Spectral Characterization of G-Quadruplex Structures and G-Quadruplex/Ligand Binding. The G-quadruplex structures are first characterized by CD spectra. For preparing a G-quadruplex with a single structure and avoiding complexity from DNA structural diversity, appropriate buffer was adopted based on the well-established structural characterizations under such conditions.[27−30] The oligonucleotides TG_4T and TBA were dissolved in K^+ buffer, respectively forming the structures of parallel four-stranded and antiparallel chair-type G-quadruplexes. Meanwhile, $AG_3(T_2AG_3)_3$ and $G_4T_4G_4$ were dissolved in Na^+ buffer, respectively forming the antiparallel basket-type and dimer-hairpin-folded antiparallel G-quadruplexes. The measured CD spectra (Figure S2) further confirm the formation of the four G-quadruplexes with the targeted conformation patterns shown in Figure S1. As shown in Figure S2, $AG_3(T_2AG_3)_3$, TBA, and $(G_4T_4G_4)2$ present a positive peak at 295 nm and a negative peak at 263 nm that is characteristic for the antiparallel G-quadruplexes, while the parallel four-stranded $(TG_4T)4$ exhibits a positive peak at 263 nm and a negative peak at 243 nm.[31]

Upon addition of TMPyP4 and incubation in the buffer, the G-quadruplex/ligand complexes are formed. A large excess of G-quadruplexes relative to the concentration of TMPyP4 were employed (molar ratio of 6:1) to ensure that each TMPyP4 molecule is bound to the G-quadruplex. As shown in Figure 1a, in the steady-state UV−vis absorption spectra, compared with free TMPyP4, red shifts from 420 to 435 nm and hypochromicity degrees of ∼35% at the Soret band maxima are observed for the complexes of G-quadruplex/TMPyP4, indicating the occurrence of the binding of TMPyP4 to the G-quadruplexes.[19] In addition, the steady-state fluorescence spectra also confirm the G-quadruplex/ligand binding, as featured by the splitting of emission into two peaks and the enhanced fluorescence intensity relative to free TMPyP4 (Figure S3).[19]

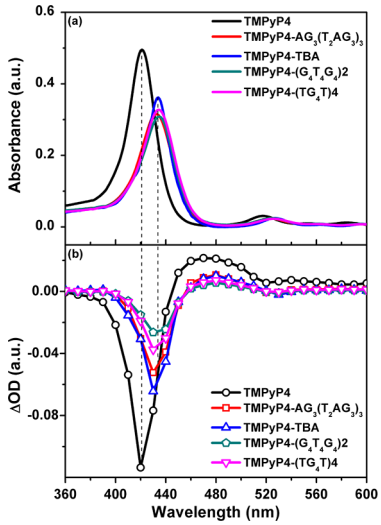

Figure 1. (a) Steady-state UV−vis absorption spectra, and (b) transient absorption spectra instantaneously (50 ns) after laser flash photolysis upon 532 nm excitation, for free TMPyP4 (2 μM) and its complexes with each of the four G-quadruplexes (12 μM) in buffer solution (10 mM Tris-HCl, 1 mM EDTA, and 100 mM KCl or NaCl, pH = 7.5).

Differentiating the Coexisting Binding Sites and Interaction Modes by the Transient Spectral Method Using the Triplet Excited State as a Reporter. After these steady-state spectral characterizations, transient UV−vis absorption spectra were measured to monitor the excited state dynamics of TMPyP4 in each of the four G-quadruplexes. The measurements were started with the simplistic conditions that each TMPyP4 is expected to be bound and there is no free ligand population in the large excess of G-quadruplex (molar ratio of 6:1), and then were extended to a series of G-quadruplex/ligand molar ratios. The results for the molar ratio of 6:1 are first discussed as follows.

Figure 1b shows the transient UV−vis absorption spectra of free TMPyP4 and TMPyP4 bound with each of the four G-quadruplexes. For free TMPyP4, transient absorptions due to triplet excited state formation (positive peak at 470 nm) and ground state depletion (negative peak at 420 nm) are observed upon 532 nm excitation. When TMPyP4 is bound to G-quadruplexes, red shifts and hypochromicity are also observed in the transient absorption spectra, for both the ground state depletion and triplet absorption bands. The triplet absorption band is red-shifted to 480 nm in the G-quadruplex/TMPyP4 complexes. Therefore, the triplet excited state decay dynamics were monitored for free TMPyP4 at 470 nm and G-quadruplex/TMPyP4 complexes at 480 nm (Figure 2).

Figure 2 displays the triplet decay curves for TMPyP4 respectively bound with the four G-quadruplexes, in comparison with free TMPyP4. As can be seen, the triplet decay of free TMPyP4 follows a monoexponential law with a lifetime of 1.6 ± 0.02 μs that matches early reports (Table 1).[32,33] This can be reasonably explained in that all porphyrin molecules are homogeneously distributed in solution as free solutes. When TMPyP4 is bound with G-quadruplexes, the triplet decay behavior becomes markedly different. As shown in Figure 2a, in the presence of $AG_3(T_2AG_3)_3$, the triplet excited states of TMPyP4 survive much longer and do not exhibit a first-order exponential decay, but follow a second-order exponential decay

dx.doi.org/10.1021/jz501040a | J. Phys. Chem. Lett. 2014, 5, 2259−2266

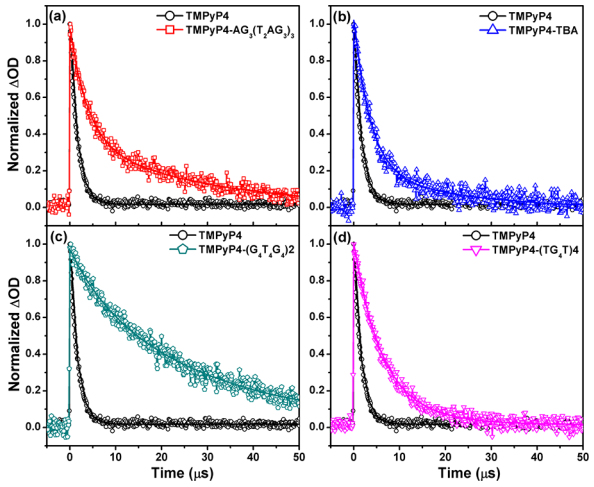

Figure 2. Normalized triplet decay signals after laser flash photolysis of TMPyP4 (2 μM) upon 532 nm excitation in the absence (black) and presence of each G-quadruplex (12 μM): (a) $AG_3(T_2AG_3)_3$ (red), (b) TBA (blue), (c) $(G_4T_4G_4)2$ (dark cyan), and (d) $(TG_4T)4$ (magenta). Fitted curves are shown by solid lines. The fits are all obtained from complete decay traces. For the sake of being comparable with other three G-quadruplexes, only partial decay traces of $(G_4T_4G_4)2$/TMPyP4 are presented in panel c, and its entire trace is provided in Figure S4.

Table 1. Triplet Decay Lifetimes of Free TMPyP4, and TMPyP4 Respectively Bound with the Four DNA G-Quadruplexes, Obtained from Biexponential Fitting ($I = I_0 + A_1e^{-t/\tau_1} + A_2e^{-t/\tau_2}$)[a]

sample	τ_1 (μs)	τ_2 (μs)
TMPyP4	1.6 ± 0.02	
TMPyP4-$AG_3(T_2AG_3)_3$	3.9 ± 0.1 (62%)	29.0 ± 0.9 (38%)
TMPyP4-TBA	3.6 ± 0.2 (79%)	23.0 ± 1.5 (21%)
TMPyP4-$(G_4T_4G_4)2$	3.6 ± 0.1 (17%)	28.0 ± 0.6 (83%)
TMPyP4-$(TG_4T)4$	3.2 ± 0.1 (29%)	12.2 ± 0.5 (71%)

[a]Pre-exponential factors for the two lifetime components yield the respective percentages of two binding modes (values shown in brackets).

with lifetimes of 3.9 ± 0.1 μs and 29.0 ± 0.9 μs (Figure 2a and Table 1). First, the disappearance of the 1.6 μs lifetime component indicates the absence of free TMPyP4 population under the large excess of G-quadruplex, as expected. Second, the two components of dramatically longer lifetimes can be attributed to slower triplet deactivation processes (relaxation to ground state by intersystem crossing), due to important restrictions in the degrees of freedom inside the G-quadruplex binding sites, where a microenvironment is provided that protects the triplet excited state from being quenched by the oxygen molecules in bulk solution.[24] In this context, the biexponential triplet decays for the bound TMPyP4 in $AG_3(T_2AG_3)_3$ should be correlated with the existence of two types of binding sites.

A schematic representation for the possible binding sites is shown in Figure 3. As a typical π-stacking ligand, TMPyP4 can stack on the face of a guanine quartet.[12] The binding involves intercalation between two neighboring G-tetrads and end-stacking of porphyrins onto the terminal G-quartets. In the end-stacking mode, only one side of porphyrin macrocycle faces the terminal G-quartet, leading to this side being shielded from the bulk solution, whereas the other side faces the TTA

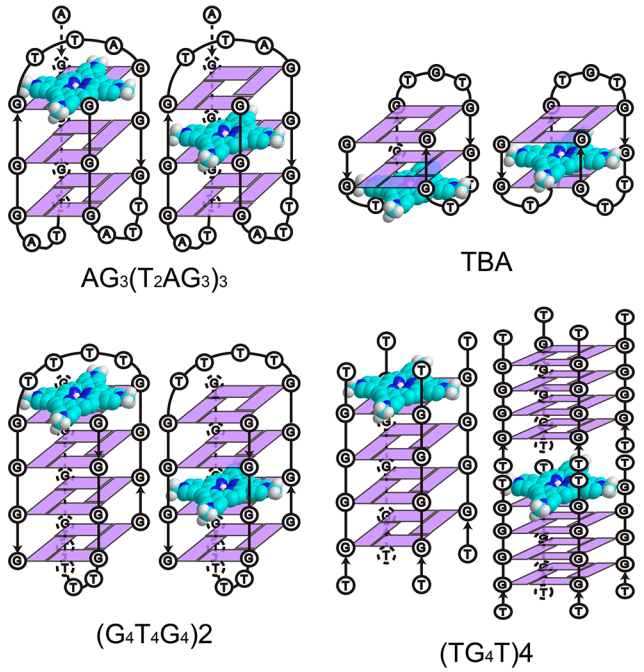

Figure 3. Anticipated binding modes of TMPyP4 with each of the four G-quadruplexes, involving end-stacking onto terminal G-quartet and intercalation between two neighboring G-tetrads. For $AG_3(T_2AG_3)_3$ and TBA, end-stacking mode within loop regions at two ends are both possible, only one pattern is depicted here, which is the end-stacking within the diagonal TTA loop for $AG_3(T_2AG_3)_3$ and the end-stacking with the two lateral TT loops for TBA. For $(G_4T_4G_4)2$, two equivalent TTTT loops are present at two ends and the end-stacking mode is identical at each end.

loop and is less shielded, allowing partial exposure to the bulk. In contrast, in the intercalation mode, both the two sides of porphyrin macrocycle are screened from the bulk, constituting a well-protected microenvironment that prevents oxygen quenching. Obviously, the intercalation mode much better protects porphyrin macrocycle from molecular oxygen access that quenches triplet excited state. The slow decay component of 29.0 ± 0.9 μs for the triplet decay is therefore assigned to the population bound in intercalation mode, while the faster decay component of 3.9 ± 0.1 μs corresponds to the population bound in end-stacking mode. Here, the possibility of charge transfer contributing to triplet quenching has been eliminated. If charge transfer between porphyrin and guanine occurs, charge separated species such as guanine cation (G^+) absorbing above 500 nm[34] should be observed in the transient spectra. However, the transient spectra at long times after photoexcitation do not show apparent signal belonging to G^+ (Figure S5). Instead, the complete recovery of ground state depletion is clearly seen. This indicates that the charge transfer is not likely to be involved in the triplet quenching.

By monitoring triplet excited state decay behaviors, our experiments clearly indicate that two binding modes—intercalation and end-stacking—simultaneously exist for TMPyP4 interacting with the human telomeric sequence $AG_3(T_2AG_3)_3$. This result sheds light on the long-standing controversy regarding the binding mode of $AG_3(T_2AG_3)_3$-TMPyP4. According to the isothermal titration calorimetry (ITC) experiment and the determined binding stoichiometry (1:2), intercalation between G-tetrads was elucidated to be the binding mode.[17] However, the photocleavage experiment

dx.doi.org/10.1021/jz501040a | J. Phys. Chem. Lett. 2014, 5, 2259−2266

showed selective cleavage at the G-tetrad near the diagonal TTA, which indicated that TMPyP4 is end-stacking in the diagonal TTA loop region.[23] However, it was also pointed out that some binding sites (i.e., intercalation) may be invisible when assayed by photocleavage, since the sequestering of porphyrin within G-tetrads may quench the photoactivating potential of TMPyP4 and thereby cannot produce an activated species required by photocleavage experiment.[23] Unlike these single technique experiments, the use of different techniques in synergy provided crucial information that could reconcile this controversial issue. By combining several experimental techniques of UV−vis absorption, fluorescence, surface-enhanced Raman (SER) and UV−vis resonance Raman (UVRR) spectroscopy, a mixed binding mode was proposed for the interaction of TMPyP4 with $AG_3(T_2AG_3)_3$, including both the end-stacking within loop regions and the intercalation between adjacent G-tetrads.[19] Interestingly, it shows in our experiments that this scenario of mixed interaction modes can be revealed readily and clearly in a single assay, by using the triplet excited state as a spectral reporter. The triplet quenching dynamics is thus demonstrated to be quite sensitive to the local bound microenvironment, allowing easy recognition of different binding sites and interaction modes in a single measurement.

As for TMPyP4 interacting with the other three distinctive G-quadruplexes, the measurements of triplet decay dynamics also offer explicit differentiation of the coexisted binding sites and modes. Figure 2b−d display the triplet decay curves of TMPyP4 in complex with TBA, $(G_4T_4G_4)2$, and $(TG_4T)4$, respectively. It is first noticeable that the biexponential decay behaviors are also exhibited, with a fast (τ_1) and a slow (τ_2) lifetime component, suggesting the simultaneous existence of two binding modes. The fitted lifetimes are listed in Table 1. The fast lifetime component (τ_1) is 3.6 ± 0.2, 3.6 ± 0.1, and 3.2 ± 0.1 μs for the binding of TMPyP4 with TBA, $(G_4T_4G_4)2$ and $(TG_4T)4$, respectively, almost identical with the value of 3.9 ± 0.1 μs for $AG_3(T_2AG_3)_3$. These short lifetime components should be ascribed to the population of end-stacking binding mode within loop regions, where the partial exposure to bulk results in relatively fast triplet quenching, as already discussed for $AG_3(T_2AG_3)_3$. The anticipated binding models are plotted in Figure 3. As can be seen, the end-stacking onto the terminal G-quartet are plausible for all of the four DNA sequences. The slightly faster lifetime component of 3.2 ± 0.1 μs for $(TG_4T)4$ is also reasonable, if considering the lack of loop protection for the parallel four-stranded structure of $(TG_4T)4$, unlike that for the other folded structures that all have loop regions at two ends.

Second, the slow decay component (τ_2) is 23.0 ± 1.5 μs and 28.0 ± 0.6 μs, respectively, for TMPyP4 bound with TBA and $(G_4T_4G_4)2$, falling into the same range as that of $AG_3(T_2AG_3)_3$. This long lifetime component is ascribed to the population bound in the intercalation mode, where TMPyP4 is intercalated between two adjacent G-tetrads and is well protected from oxygen quenching. However, for TMPyP4 associated with the parallel four-stranded structure of $(TG_4T)4$, the slow decay component (τ_2) is 12.2 ± 0.2 μs, much shorter than the typical intercalative lifetime (23−29 μs) but longer than the typical end-stacking lifetime (3−4 μs). This indicates a new type of binding mode, which was previously proposed as the sandwich-type binding mode.[35] As shown in Figure 3, vertical stacking of two $(TG_4T)4$ can form the G-quadruplex dimer structure, where the ligand is clamped in a tail-to-tail fashion between the 3′-end tetrads of two $(TG_4T)4$ monomers. Such a sandwich-type binding mode can offer an additional protection for the side of porphyrin exposed to bulk solution, but with less restriction and much more freedom compared with the intercalation mode. Therefore, the triplet decay lifetime corresponding to the sandwich-type binding mode lies in between those for the typical end-stacking and intercalation modes, as observed here. Under our experimental condition, the large excess of G-quadruplex concentration can promote the stacking of two $(TG_4T)4$ monomers, which rationally explains the existence of the sandwich-type binding mode. For $(TG_4T)4$, the lack of typical intercalation binding mode observed here is in good agreement with previous reports.[19,22,23,36] The specific parallel highly ordered structure of $(TG_4T)4$ may favor the strong end-stacking binding mode, without the disruption to the phosphate backbones, which is distinctive from the other three G-quadruplex structures.

Assessing the Distribution of Coexisting Binding Modes by the Transient Spectral Method Using the Triplet Excited State as a Reporter. In addition to explicitly differentiating the coexisted binding sites and interaction modes, the triplet reporter method can further assess contributions of different binding interactions. In the biexponential fitting equation, the pre-exponential factors obtained for the two lifetime components actually correspond to the respective percentages of the two binding modes, and these values are also listed in Table 1 (in brackets). This demonstrates for the first time the relative contributions of the coexisted binding modes for each of the four G-quadruplex structures. At the molar ratio of 6:1, it shows in Table 1 that end-stacking is the preferred binding mode for $AG_3(T_2AG_3)_3$ (62%) and TBA(79%), while intercalation is the dominant binding mode for $(G_4T_4G_4)2$ (83%). For $(TG_4T)4$, end-stacking accounts for 29%, and the sandwich-type binding mode accounts for 71%. Such information was unknown before and could not possibly be obtained by conventional techniques.[12]

A series of experiments were also performed under different molar ratios of [G-quadruplex]/[ligand], as those for 6:1. The triplet decay curves are displayed in Figure S6 and the fitted percentages of binding modes are plotted in Figure 4. For $(TG_4T)4$, it can be seen that the sandwich-type binding mode becomes dominant over the end-stacking mode with the increased [G-quadruplex]/[ligand] ratio, which is reasonable because the high G-quadruplex concentration can facilitate the stacking of two $(TG_4T)4$ monomers and thus the sandwich-type binding. For $AG_3(T_2AG_3)_3$, TBA, and $(G_4T_4G_4)2$, when comparing the occupation level of the two coexisted binding sites, the trend clearly shows that around the [G-quadruplex]/[ligand] ratio of 1:1, the binding is all dominated by the end-stacking mode. Progressive increase of the [G-quadruplex]/[ligand] ratio (1:1, 2:1, 4:1, 6:1) results in gradual decrease of the end-stacking percentage and increase of intercalation percentage, particularly for $(G_4T_4G_4)2$, intercalation even becomes the major binding mode under the 4:1 and 6:1 conditions.

For the π-stacking ligand TMPyP4 interacting with G-quadruplexes, it is generally assumed that end-stacking is the preferred binding site with high affinity, whereas the intercalation mode has relatively low stability.[22,23,36] Under this assumption, it was also postulated that with the great excess of G-quadruplex, TMPyP4 is expected to exclusively locate at the high affinity binding sites (i.e., end-stacking).[22] The results (Figure 4) obtained here provide new insights in two aspects:

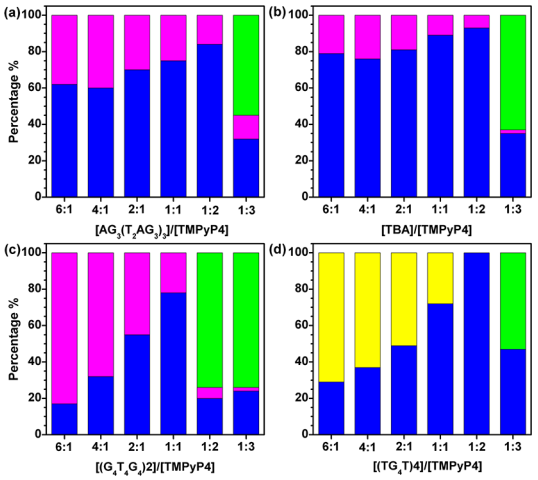

Figure 4. Histogram plots for the population percentage of free TMPyP4 (green), TMPyP4 bound in the intercalation mode (magenta), TMPyP4 bound in the end-stacking mode (blue), and TMPyP4 bound in the sandwich mode (yellow), obtained for different [G-quadruplex]/[TMPyP4] molar ratios of 6:1, 4:1, 2:1, 1:1, 1:2, and 1:3.

(1) even in the large excess of G-quadruplex concentration, there are two binding sites and the ligand population is not homogeneous, and (2) the high affinity end-stacking mode is the preferred binding site when the concentrations of G-quadruplex and ligand are comparable, whereas the less favored intercalation mode can be enhanced in the large excess of G-quadruplex. Particularly for $(G_4T_4G_4)2$, the enhanced population of the intercalation mode is significant at high ratios of [G-quadruplex]/[ligand], which might be associated with its unique structure.

It is also shown in Figure 4 that the ligand binding reaches saturation and free TMPyP4 population emerges at a certain [G-quadruplex]/[TMPyP4] ratio when the ligand is in excess (1:2 or 1:3). In this case, the triplet lifetime of free TMPyP4 (1.6 μs) is necessary to be included to obtain a good fitting of the decay signal. For $AG_3(T_2AG_3)_3$, TBA, and $(G_4T_4G_4)2$, three lifetime components corresponding to free, end-stacking, and intercalation populations are required for the fitting. For $(TG_4T)4$ at its low concentration, the possibility forming $(TG_4T)4$ dimer and thus the sandwich-type binding is negligible, two lifetime values corresponding to free and end-stacking population are thus required for the fitting.

Revealing the Binding Behavior Change by the Transient Spectral Method Using the Triplet Excited State as a Reporter. To further testify the sensitivity of this method, we performed control experiments to examine the binding behavior variation induced by the G-quadruplex structural change. It is well-known that G-quadruplex structure can be influenced by the metal cation K^+ or Na^+ in buffer solution.[27,29] In particular, the folded G-quadruplexes of $AG_3(T_2AG_3)_3$ and $(G_4T_4G_4)2$ present diverse structures in buffer containing either Na^+ or K^+. For these two G-quadruplexes upon structural change from Na^+ buffer to K^+ buffer, the triplet decay dynamics of the bound TMPyP4 were measured, and the results are displayed in Figure 5.

For $AG_3(T_2AG_3)_3$, as shown in Figure 5c, there is only one single basket-type structure when prepared in Na^+ buffer, whereas in K^+ buffer, two conformations exist, including the major hybrid-type (parallel/antiparallel mixed folding topology) and the minor basket-type.[27] Such structural change is likely to invoke the alteration of ligand binding. Indeed, a different triplet decay rate is observed for TMPyP4 bound with the Na^+ or K^+ buffered $AG_3(T_2AG_3)_3$, as shown in Figure 5a. From biexponential fitting, it is found that the relative contribution of the intercalation mode is greatly increased to about 61% in K^+ solution, which is about 2.4 times larger than the result (25%) obtained in Na^+ solution (Inset of Figure 5a). The increased percentage of intercalation mode in K^+ solution is presumably caused by the presence of the hybrid-type conformation, which possesses a distinct folding topology, consisting of three G-tetrads connected consecutively with a double-chain-reversal side loop and two lateral loops. This is unlike the basket-type structure in Na^+ that has diagonal TTA loop to stabilize the end-stacking binding mode.[19,22] It is anticipated then that the end-stacking binding mode is not favored as much, and thus intercalation becomes the dominant binding mode for the hybrid-type conformation in K^+.

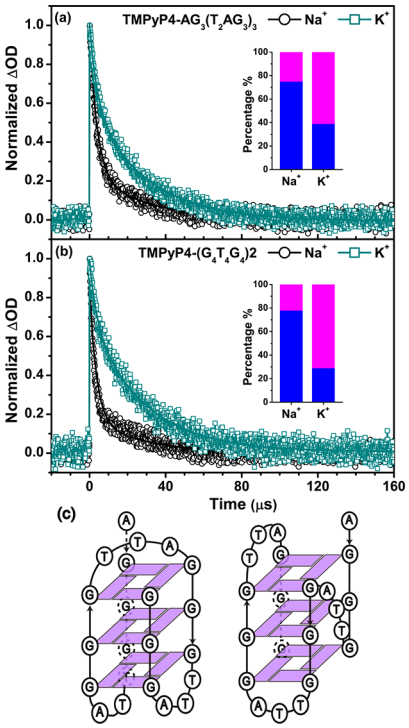

Figure 5. Normalized triplet decay signals after 523 nm laser flash photolysis of TMPyP4 (2 μM) in the presence of 2 μM of (a) $AG_3(T_2AG_3)_3$ in Na^+ buffer (black circle) or K^+ buffer (green square), and (b) $(G_4T_4G_4)2$ in Na^+ buffer (black circle) or K^+ buffer (green square). The derived binding mode percentage is shown in the insets. (c) Schematic topology diagrams for $AG_3(T_2AG_3)_3$ in the form of basket-type (left) and hybrid-type (right).

For another G-quadruplex $(G_4T_4G_4)2$, its structure (Figure S1) in Na^+ solution is very similar to that in K^+ solution, with the only difference being the distance between the diagonal TTTT loop and the terminal G-quartet, according to NMR studies.[29] Since the diagonal TTTT loop regions at the end appear to be less extended in the K^+ solution, it is expected that TMPyP4 has less possibility to be accommodated in the end-stacking mode. Accordingly, by monitoring the triplet decay dynamics (Figure 5b), we observe that the percentage of the end-stacking mode in K^+ is decreased to ~29%, which is about 2.7 times smaller than that in Na^+ solution (78%), as shown in Figure 5b inset. It is demonstrated here that the binding

dx.doi.org/10.1021/jz501040a | J. Phys. Chem. Lett. 2014, 5, 2259−2266

interaction varied with the small structural change of G-quadruplex can still be sensitively captured by following the triplet decay dynamics.

In conclusion, the fact that triplet excited states as reporters can probe interactions of TMPyP4 with four representing important telomeric G-quadruplexes—$AG_3(T_2AG_3)_3$, TBA, $(G_4T_4G_4)2$, and $(TG_4T)4$—is convincingly demonstrated in this work: (1) By following triplet decay dynamics that are sensitive to the local bound microenvironment, coexisted binding sites and interaction modes are explicitly differentiated, as featured by their respective lifetime components of 3−4 μs, 23−29 μs, and 12 μs for end-stacking within loop regions, intercalation between adjacent G-tetrads, and sandwich between two monomer G-quadruplexes; (2) Further, triplet decay analysis determines the relative contributions of each of the coexisted binding modes. The results provide new insights to understand G-quadruplex/TMPyP4 interaction, showing that the high affinity end-stacking mode is the preferred binding site when the concentrations of G-quadruplex and ligand are comparable, whereas the low stability intercalation mode can be enhanced in the large excess of G-quadruplex concentration, particularly for $(G_4T_4G_4)2$, intercalation even becomes the major binding mode; (3) Control experiments corroborate further the sensitivity of this method, which can even capture the binding behavior change as the G-quadruplex structures are adjusted by Na^+ or K^+.

With the transient method of triplet excited states as spectral reporters, the coexisted binding sites are allowed to be recognized and distinguished in a single assay, revealing the full scenario of mixed interaction modes and determining their respective distributions that could not possibly be obtained by conventional methods. This new method thus provides a straightforward and efficient platform to monitor and differentiate the versatile and complex G-quadruplex/ligand interactions, which is a difficult task and usually requires a combination of several different techniques. Importantly, since various ligand binding modes play crucial roles in stabilizing G-quadruplex structures, recognizing and further assessing contributions of these interactions, as implemented here with the triplet reporter method, is essential for the rational design of G-quadruplex ligands that can be developed as novel anticancer drugs. We also expect substantial potential for this new triplet reporter method exploited in conjunction with other structural characterization techniques (such as CD, X-ray, and NMR), and hope to arouse the interests of further related work.

EXPERIMENTAL METHODS

Materials. The DNA oligonucleotides TBA, $AG_3(T_2AG_3)_3$, TG_4T, and $G_4T_4G_4$ were purchased from the SBS Genetech Co., Ltd. (China) in the PAGE-purified form. Single-strand concentrations were determined by monitoring the absorbance at 260 nm in the UV−vis spectra and using the corresponding extinction coefficients of 1.433×10^5, 2.285×10^5, 0.578×10^5 and 1.152×10^5 $M^{-1}cm^{-1}$ for TBA, $AG_3(T_2AG_3)_3$, TG_4T, and $G_4T_4G_4$, respectively.[37] To prepare G-quadruplexes with the targeted structures, the oligonucleotides were dissolved in a buffer solution containing 10 mM Tris-HCl, 1 mM EDTA, and 100 mM KCl for TG4T and TBA or 100 mM NaCl for $AG_3(T_2AG_3)_3$ and $(G_4T_4G_4)2$ at pH 7.5. The mixture was then heated to 95 °C for 5 min, cooled down to room temperature with a cooling rate of 0.5 °C/min, and then incubated at 4 °C for 12 h.

The porphyrin derivative 5,10,15,20-tetrakis(*N*-methylpyridinium-4-yl)-21H,23H-porphyrin (TMPyP4) in the form of tetra-*p*-tosylate salt was purchased from Tokyo Chemical Industry (TCI) and used as received. A 0.5 mM TMPyP4 stock solution in ultrapure water (18.2 MΩ, purified by Millipore filtration) was stored in the dark at −20 °C to prevent photodegradation. In the experiment, freshly diluted TMPyP4 buffer solution (10 mM Tris-HCl, 1 mM EDTA, and 100 mM KCl or 100 mM NaCl at pH 7.5) with 2 μM concentration of TMPyP4 was used. The concentration of TMPyP4 was determined by measuring its absorbance at 424 nm in the UV−vis spectra with an extinction coefficient of 2.26×10^5 $M^{-1}cm^{-1}$.[38]

Steady-State Spectral Measurements. Circular dichroism spectra of the four G-quadruplexes (10 μM) were recorded at room temperature on a Jasco J-815 spectropolarimeter. Each measurement was collected from 320 to 200 nm at a scan speed of 500 nm/min with a response time of 0.5 s. The final spectra were the average of three repetitions. The spectrum from a blank sample containing only buffer was used as the background, which was subtracted from the averaged spectra. UV−vis absorption spectra were recorded in the 360−600 nm range with a UV−vis spectrometer (model U-3010, Hitachi). Fluorescence spectra were measured with a fluorescence spectrometer (F4600, Hitachi) at the excitation wavelength of 532 nm. Quartz cuvettes of 1 cm path length were used for all steady-state spectral measurements.

Laser Flash Photolysis. The transient UV−vis absorption spectra and triplet excited state decay dynamics were measured by a nanosecond time-resolved laser flash photolysis (LFP) setup that has been described previously.[39] Briefly, the instrument comprises an Edinburgh LP920 spectrometer (Edinburgh Instrument Ltd.) combined with an Nd:YAG laser (Surelite II,Continuum Inc.). The excitation wavelength is 532 nm laser pulse from Q-switched Nd:YAG laser (1 Hz, fwhm ≈7 ns, 10 mJ/pulse). The analyzing light was from a 450 W pulsed xenon lamp. A monochromator equipped with a photomultiplier for collecting the spectral range from 350 to 850 nm was used to analyze transient absorption spectra. The signals from the photomultiplier were displayed and recorded as a function of time on a 100 Hz (1.25 Gs/s sampling rate) oscilloscope (Tektronix, TDS 3012B), and the data were transferred to a personal computer. Data were analyzed by the online software of the LP920 spectrophotometer. The fitting quality was judged by weighted residuals and reduced χ^2 value.

Samples of G-quadruplexes and TMPyP4 were mixed before each measurement, by adding G-quadruplex DNA stock solution to the freshly diluted TMPyP4 buffer solution, and the mixture was incubated at room temperature for 30 min to ensure good binding. In the mixed solution, the concentration of TMPyP4 was fixed at a low concentration of 2 μM, so that prophyrins were maintained under monomeric form without aggregation, and the G-quadruplex concentration varied from zero to 12 μM for the serial experiments. All solutions subject to measurements were under the air-saturated conditions. All measurements were carried out in 1 cm path length quartz cuvettes at room temperature.

ASSOCIATED CONTENT

Supporting Information

Structures of TMPyP4 and schematic topology diagrams for the four G-quadruplexes, CD spectra, fluorescence spectra, transient spectra at long times and triplet decay curves at

dx.doi.org/10.1021/jz501040a | J. Phys. Chem. Lett. 2014, 5, 2259−2266

various [G-quadruplex]/[ligand] molar ratios. This material is available free of charge via the Internet at http://pubs.acs.org.

AUTHOR INFORMATION

Corresponding Author

*E-mail: hongmei@iccas.ac.cn.

Notes

The authors declare no competing financial interest.

ACKNOWLEDGMENTS

This work was financially supported by the National Natural Science Foundation of China (Grant No. 21333012, 21373233), the National Basic Research Program of China (2013CB834602), and the Chinese Academy of Sciences (Project XDB12020200).

REFERENCES

(1) Huppert, J. L. Four-Stranded Nucleic Acids: Structure, Function and Targeting of G-Quadruplexes. *Chem. Soc. Rev.* **2008**, *37*, 1375−1384.

(2) Röttger, K.; Schwalb, N. K.; Temps, F. Electronic Deactivation of Guanosine in Extended Hydrogen-Bonded Self-Assemblies. *J. Phys. Chem. A* **2013**, *117*, 2469−2478.

(3) Changenet-Barret, P.; Emanuele, E.; Gustavsson, T.; Improta, R.; Kotlyar, A. B.; Markovitsi, D.; Vaya, I.; Zakrzewska, K.; Zikich, D. Optical Properties of Guanine Nanowires: Experimental and Theoretical Study. *J. Phys. Chem. C* **2010**, *114*, 14339−14346.

(4) Hua, Y.; Changenet-Barret, P.; Improta, R.; Vaya, I.; Gustavsson, T.; Kotlyar, A. B.; Zikich, D.; Sket, P.; Plavec, J.; Markovitsi, D. Cation Effect on the Electronic Excited States of Guanine Nanostructures Studied by Time-Resolved Fluorescence Spectroscopy. *J. Phys. Chem. C* **2012**, *116*, 14682−14689.

(5) Hua, Y.; Changenet-Barret, P.; Gustavsson, T.; Markovitsi, D. The Effect of Size on the Optical Properties of Guanine Nanostructures: A Femtosecond to Nanosecond Study. *Phys. Chem. Chem. Phys.* **2013**, *15*, 7396−7402.

(6) Biffi, G.; Tannahill, D.; McCafferty, J.; Balasubramanian, S. Quantitative Visualization of DNA G-Quadruplex Structures in Human Cells. *Nat. Chem.* **2013**, *5*, 182−186.

(7) Lam, E. Y. N.; Beraldi, D.; Tannahill, D.; Balasubramanian, S. G-Quadruplex Structures Are Stable and Detectable in Human Genomic DNA. *Nat. Commun.* **2013**, *4*, 1796.

(8) Collie, G. W.; Parkinson, G. N. The Application of DNA and RNA G-Quadruplexes to Therapeutic Medicines. *Chem. Soc. Rev.* **2011**, *40*, 5867−5892.

(9) McLuckie, K. I. E.; Di Antonio, M.; Zecchini, H.; Xian, J.; Caldas, C.; Krippendorff, B.-F.; Tannahill, D.; Lowe, C.; Balasubramanian, S. G-Quadruplex DNA as a Molecular Target for Induced Synthetic Lethality in Cancer Cells. *J. Am. Chem. Soc.* **2013**, *135*, 9640−9643.

(10) Georgiades, S. N.; Abd Karim, N. H.; Suntharalingam, K.; Vilar, R. Interaction of Metal Complexes with G-Quadruplex DNA. *Angew. Chem., Int. Ed.* **2010**, *49*, 4020−4034.

(11) Seenisamy, J.; Bashyam, S.; Gokhale, V.; Vankayalapati, H.; Sun, D.; Siddiqui-Jain, A.; Streiner, N.; Shin-ya, K.; White, E.; Wilson, W. D.; et al. Design and Synthesis of an Expanded Porphyrin That Has Selectivity for the c-MYC G-Quadruplex Structure. *J. Am. Chem. Soc.* **2005**, *127*, 2944−2959.

(12) Murat, P.; Singh, Y.; Defrancq, E. Methods for Investigating G-Quadruplex DNA/Ligand Interactions. *Chem. Soc. Rev.* **2011**, *40*, 5293−5307.

(13) Jaumot, J.; Gargallo, R. Experimental Methods for Studying the Interactions between G-Quadruplex Structures and Ligands. *Curr. Pharm. Des.* **2012**, *18*, 1900−1916.

(14) Koirala, D.; Dhakal, S.; Ashbridge, B.; Sannohe, Y.; Rodriguez, R.; Sugiyama, H.; Balasubramanian, S.; Mao, H. A Single-Molecule Platform for Investigation of Interactions between G-Quadruplexes and Small-Molecule Ligands. *Nat. Chem.* **2011**, *3*, 782−787.

(15) Parkinson, G. N.; Ghosh, R.; Neidle, S. Structural Basis for Binding of Porphyrin to Human Telomeres. *Biochemistry* **2007**, *46*, 2390−2397.

(16) Phan, A. T.; Kuryavyi, V.; Gaw, H. Y.; Patel, D. J. Small-Molecule Interaction with a Five-Guanine-Tract G-Quadruplex Structure from the Human Myc Promoter. *Nat. Chem. Biol.* **2005**, *1*, 167−173.

(17) Haq, I.; Trent, J. O.; Chowdhry, B. Z.; Jenkins, T. C. Intercalative G-Tetraplex Stabilization of Telomeric DNA by a Cationic Porphyrin. *J. Am. Chem. Soc.* **1999**, *121*, 1768−1779.

(18) Martino, L.; Pagano, B.; Fotticchia, I.; Neidle, S.; Giancola, C. Shedding Light on the Interaction between TMPyP4 and Human Telomeric Quadruplexes. *J. Phys. Chem. B* **2009**, *113*, 14779−14786.

(19) Wei, C.; Jia, G.; Yuan, J.; Feng, Z.; Li, C. A Spectroscopic Study on the Interactions of Porphyrin with G-Quadruplex DNAs. *Biochemistry* **2006**, *45*, 6681−6691.

(20) Jain, A. K.; Reddy, V. V.; Paul, A.; K, M.; Bhattacharya, S. Synthesis and Evaluation of a Novel Class of G-Quadruplex-Stabilizing Small Molecules Based on the 1,3-Phenylene-Bis(Piperazinyl Benzimidazole) System. *Biochemistry* **2009**, *48*, 10693−10704.

(21) Kimura, T.; Kawai, K.; Fujitsuka, M.; Majima, T. Detection of the G-Quadruplex-TMPyP4 Complex by 2-Aminopurine Modified Human Telomeric DNA. *Chem. Commun.* **2006**, 401−402.

(22) Jia, G.; Feng, Z.; Wei, C.; Zhou, J.; Wang, X.; Li, C. Dynamic Insight into the Interaction between Porphyrin and G-Quadruplex DNAs: Time-Resolved Fluorescence Anisotropy Study. *J. Phys. Chem. B* **2009**, *113*, 16237−16245.

(23) Han, H.; Langley, D. R.; Rangan, A.; Hurley, L. H. Selective Interactions of Cationic Porphyrins with G-Quadruplex Structures. *J. Am. Chem. Soc.* **2001**, *123*, 8902−8913.

(24) Jimenez, M. C.; Miranda, M. A.; Vaya, I. Triplet Excited States as Chiral Reporters for the Binding of Drugs to Transport Proteins. *J. Am. Chem. Soc.* **2005**, *127*, 10134−10135.

(25) Pérez-Ruiz, R.; Bueno, C. J.; Jiménez, M. C.; Miranda, M. A. In Situ Transient Absorption Spectroscopy to Assess Competition between Serum Albumin and Alpha-1-Acid Glycoprotein for Drug Transport. *J. Phys. Chem. Lett.* **2010**, *1*, 829−833.

(26) Siddiqui-Jain, A.; Grand, C. L.; Bearss, D. J.; Hurley, L. H. Direct Evidence for a G-Quadruplex in a Promoter Region and Its Targeting with a Small Molecule to Repress c-MYC Transcription. *Proc. Natl. Acad. Sci. U.S.A.* **2002**, *99*, 11593−11598.

(27) Ambrus, A.; Chen, D.; Dai, J.; Bialis, T.; Jones, R. A.; Yang, D. Human Telomeric Sequence Forms a Hybrid-Type Intramolecular G-Quadruplex Structure with Mixed Parallel/Antiparallel Strands in Potassium Solution. *Nucleic Acids Res.* **2006**, *34*, 2723−2735.

(28) Aboul-ela, F.; Murchie, A. I. H.; Norman, D. G.; Lilley, D. M. J. Solution Structure of a Parallel-Stranded Tetraplex Formed by d(TG4T) in the Presence of Sodium Ions by Nuclear Magnetic Resonance Spectroscopy. *J. Mol. Biol.* **1994**, *243*, 458−471.

(29) Schultze, P.; Hud, N. V.; Smith, F. W.; Feigon, J. The Effect of Sodium, Potassium and Ammonium Ions on the Conformation of the Dimeric Quadruplex Formed by the *Oxytricha nova* Telomere Repeat Oligonucleotide d(G4T4G4). *Nucleic Acids Res.* **1999**, *27*, 3018−3028.

(30) Russo Krauss, I.; Merlino, A.; Giancola, C.; Randazzo, A.; Mazzarella, L.; Sica, F. Thrombin−Aptamer Recognition: A Revealed Ambiguity. *Nucleic Acids Res.* **2011**, *39*, 7858−7867.

(31) Paramasivan, S.; Rujan, I.; Bolton, P. H. Circular Dichroism of Quadruplex DNAs: Applications to Structure, Cation Effects and Ligand Binding. *Methods* **2007**, *43*, 324−331.

(32) Kruk, N. N.; Dzhagarov, B. M.; Galievsky, V. A.; Chirvony, V. S.; Turpin, P. Y. Photophysics of the Cationic 5,10,15,20-Tetrakis(4-N-Methylpyridyl) Porphyrin Bound to DNA, [Poly(dA-dT)]2 and [Poly(dG-dC)]2: Interaction with Molecular Oxygen Studied by Porphyrin Triplet−Triplet Absorption and Singlet Oxygen Luminescence. *J. Photochem. Photobiol. B:Biol.* **1998**, *42*, 181−190.

(33) Reddi, E.; Ceccon, M.; Valduga, G.; Jori, G.; Bommer, J. C.; Elisei, F.; Latterini, L.; Mazzucato, U. Photophysical Properties and Antibacterial Activity of Meso-Substituted Cationic Porphyrins. *Photochem. Photobiol.* **2002**, *75*, 462−470.

(34) Kobayashi, K.; Tagawa, S. Direct Observation of Guanine Radical Cation Deprotonation in Duplex DNA Using Pulse Radiolysis. *J. Am. Chem. Soc.* **2003**, *125*, 10213−10218.
(35) Anantha, N. V.; Azam, M.; Sheardy, R. D. Porphyrin Binding to Quadruplexed T4G4. *Biochemistry* **1998**, *37*, 2709−2714.
(36) Wheelhouse, R. T.; Sun, D.; Han, H.; Han, F. X.; Hurley, L. H. Cationic Porphyrins as Telomerase Inhibitors: The Interaction of Tetra-(*N*-Methyl-4-Pyridyl)Porphine with Quadruplex DNA. *J. Am. Chem. Soc.* **1998**, *120*, 3261−3262.
(37) Cantor, C. R.; Warshaw, M. M.; Shapiro, H. Oligonucleotide Interactions III. Circular Dichroism Studies of Conformation of Deoxyoligonucleotides. *Biopolymers* **1970**, *9*, 1059−1077.
(38) Pasternack, R. F.; Gibbs, E. J.; Villafranca, J. J. Interactions of Porphyrins with Nucleic-Acids. *Biochemistry* **1983**, *22*, 2406−2414.
(39) Yang, W.; Liu, K.; Song, D.; Du, Q.; Wang, R.; Su, H. Aggregation-Induced Enhancement Effect of Gold Nanoparticles on Triplet Excited State. *J. Phys. Chem. C* **2013**, *117*, 27088−27095.